Pyrazole Urea-Based Inhibitors of p38 MAP Kinase: From Lead Compound to Clinical Candidate

John Regan,*[,†] Steffen Breitfelder,[†] Pier Cirillo,[†] Thomas Gilmore,[†] Anne G. Graham,[‡] Eugene Hickey,[†] Bernhard Klaus,[†] Jeffrey Madwed,[§] Monica Moriak,[†] Neil Moss,[†] Chris Pargellis,[‡] Sue Pav,[‡] Alfred Proto,[‡] Alan Swinamer,[†] Liang Tong,[†] and Carol Torcellini[§]

Departments of Medicinal Chemistry, Biology, and Pharmacology, Boehringer Ingelheim Pharmaceuticals, Research and Development Center, 900 Ridgebury Road, Ridgefield, Connecticut 06877

We report on a series of N-pyrazole, N′-aryl ureas and their mode of binding to p38 mitogen activated protein kinase. Importantly, a key binding domain that is distinct from the adenosine 5′-triphoshate (ATP) binding site is exposed when the conserved activation loop, consisting in part of Asp168-Phe169-Gly170, adopts a conformation permitting lipophilic and hydrogen bonding interactions between this class of inhibitors and the protein. We describe the correlation of the structure−activity relationships and crystallographic structures of these inhibitors with p38. In addition, we incorporated another binding pharmacophore that forms a hydrogen bond at the ATP binding site. This modification affords significant improvements in binding, cellular, and in vivo potencies resulting in the selection of **45** (BIRB 796) as a clinical candidate for the treatment of inflammatory diseases.

Introduction

The proinflammatory cytokines tumor necrosis factor-α (TNF-α) and interleukin-1β (IL-1β) help regulate the body's response to infections and cellular stresses.[1] However, the pathophysiological consequences resulting from chronic and excessive production of TNF-α and IL-1β are believed to underlie the progression of many inflammatory diseases such as rheumatoid arthritis (RA),[2] Crohn's disease, inflammatory bowel disease, and psoriasis.[3] Recent data from clinical trials have secured the continued use of the soluble TNF-α receptor fusion protein, etanercept, or the chimeric TNF-α antibody, infliximab, in the treatment of RA[4−8] and Crohn's disease.[9,10] The signal transduction pathway leading to the production of TNF-α from stimulated inflammatory cells, while not fully understood, has been shown to be, in part, regulated by p38 mitogen activated protein (MAP) kinase.[11] p38 MAP kinase belongs to a group of serine/threonine kinases that includes c-Jun NH₂-terminal kinase (JNK) and extracellular-regulated protein kinase (ERK).[12] Upon extracellular stimulation by a variety of conditions and agents,[13] p38 is activated through bis-phosphorylation on a Thr-Gly-Tyr motif located in the activation loop. Activation is achieved by dual-specificity serine/threonine MAPK kinases, MKK3 and MKK6. Once activated, p38 can phosphorylate and activate other kinases or transcription factors leading to stabilized mRNA and an increase or decrease in the expression of certain target genes.[14−17]

In addition to the discovery of this important signal transduction pathway, pyridinyl imidazole **1** (SB 203580)[11] and analogues[18−22] have been identified as potent and selective inhibitors of p38 MAP kinase. Compound **1** was shown to be an effective orally active agent in several animal models of acute and chronic inflammation.[23] Recently, an analogue of **1**, compound **2** (SB 242235), inhibited endotoxin-induced ex vivo production of TNF-α and IL-1β in human clinical trials.[24] The interest in p38 as a viable target for drug intervention has escalated as a result of these early disclosures. In addition to a plethora of patent applications on imidazole-based compounds,[25−27] several journal papers have described strategies for the modification of **1**, by either the addition of other substituents to the imidazole or its replacement with different heterocycles. These endeavors have produced imidazoles **3**[28] and **4** (RPR200765A),[29] a pyrrole analogue of **1**,[30] oxazole **5**,[31] and pyrrolo[2,3-b]pyridine **6** (RWJ 68354).[32] Imidazole **7** (RWJ 67657)[33] was described to inhibit LPS-stimulated TNF-α production in human clinical trials.[34] Also, compounds with different structural features as compared to **1** have been reported as p38 inhibitors. These include, among others, **8** (VX-745)[35] and N,N-diaryl urea **8a**[36] as well as pyrazole ketone **9** (RO3201195)[37] and pyrimido[4,5-d]pyrimidinone **10**.[38] Indole amide **11** represents another group of p38 inhibitors.[39] A benzophenone class of p38 inhibitors, an example shown as **12** (EO1428), has recently been described.[40] Diamides (**13**) are disclosed as p38 inhibitors[41] (Chart 1).

Our focus in cytokine-regulated approaches to inflammatory diseases prompted us to evaluate the potential of p38 MAP kinase as a therapeutic target. Toward this

---

* To whom correspondence should be addressesd. Tel.: (203)798-4768. Fax: (203)791-6072. E-mail: jregan@rdg.boehringer-ingelheim.com.
† Department of Medicinal Chemistry.
‡ Department of Biology.
§ Department of Pharmacology.

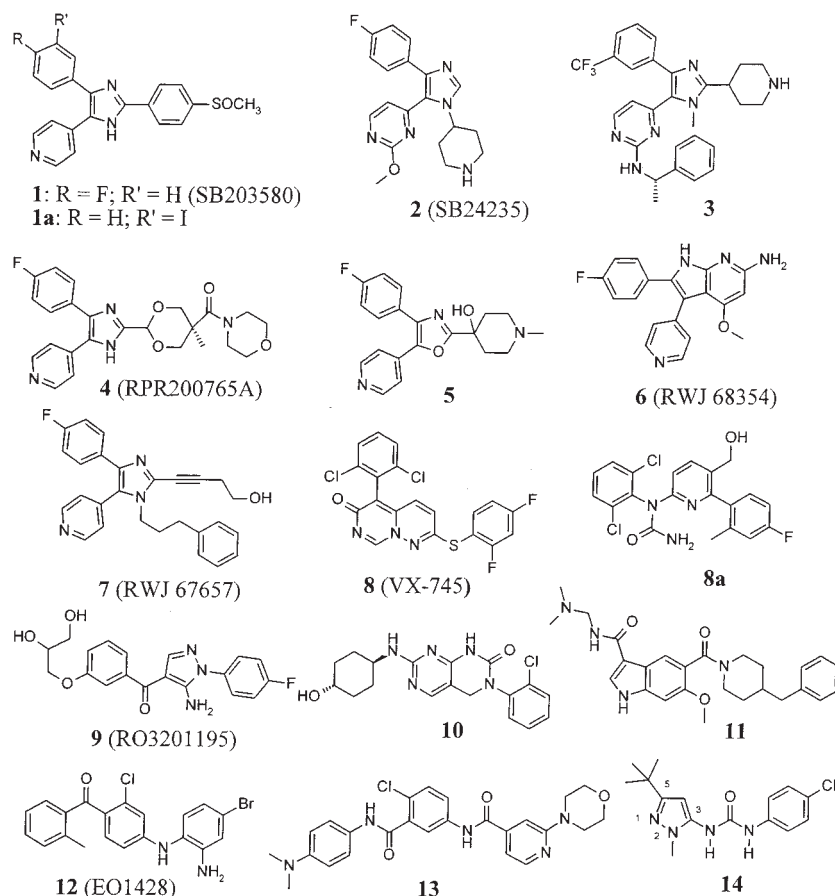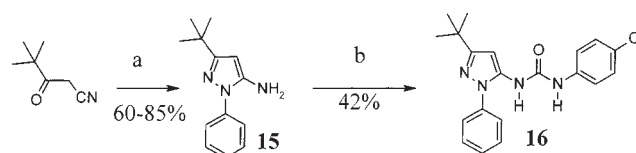**Chart 1.** Structural Classes of p38 MAP Kinase Inhibitors

1: R = F; R' = H (SB203580)
1a: R = H; R' = I

2 (SB24235)

3

4 (RPR200765A)

5

6 (RWJ 68354)

7 (RWJ 67657)

8 (VX-745)

8a

9 (RO3201195)

10

11

12 (EO1428)

13

14

Table 1. Substitution at Pyrazole N-2

compound	R	R'	K_d (nM)	Inhibition of TNF-α in THP-1 cells EC_{50} (nM)	anal.
1	--	--	10	60	--
14	CH_3	Cl	350	5,900	--
16	phenyl	Cl	8	1,000	C,H,N
46	phenyl	H	13	730	C,H,N
47	cyclo-C_6H_{11}	H	500	nd[a]	C,H,N
48	2-methylphenyl	H	200	2,300	C,H,N
49	3-methylphenyl	H	2	380	C,H,N
50	4-methylphenyl	H	3	180	C,H,N
51	3,4-dimethylphenyl	H	4	120	C,H,N
52	2-naphthyl	H	8	1,900	C,H,N
53	3-NH_2-phenyl	H	25	1,300	C,H,N
54	4-NH_2-phenyl	H	7	630	C,H,N
55	3-methoxyphenyl	H	19	960	C,H,N
56	4-methoxyphenyl	H	31	1,600	C,H,N
57	4-pyridinyl	H	21	820	C,H,N

[a] not determined

end, compound **14** was identified from high throughput screening. Reports on utilizing this compound as a lead have been disclosed.[42−44] While **14** showed only a modest binding affinity for human p38 MAP kinase (K_d = 350 nM) (Table 1), our interest in this molecule further
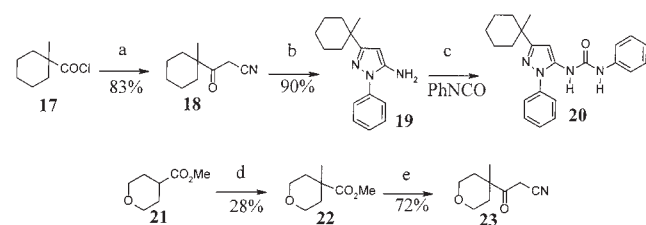
Scheme 1[a]

14, coupled with its distinction as a new structural type of inhibitor vs others (e.g., **1−13**) prompted us to undertake a systematic evaluation of its pharmacophores. The structure−activity relationships (SAR) for this class of compounds and their correlation to structural data, which led to the discovery of the clinical candidate BIRB 796,[45] are the subjects of this paper.

Chemistry

Modifications to the 2-position of the pyrazole nucleus were prepared as shown in Scheme 1 using **16** as a representative example of the compounds in Table 1. The assembly of pyrazole nucleus **15** involved the condensation of phenylhydrazine and 4,4-dimethyl-3-oxopentanenitrile in either toluene or aqueous HCl in ethanol at reflux. Urea formation was accomplished with **15** and 4-chlorophenyl isocyanate to produce **16**. For examples in Table 1 requiring noncommercially available aryl hydrazines, the method of Demers[46] was

Table 2. Substitution at Pyrazole C-5

| compound	R	K_d (nM)	anal.	compound	R	K_d (nM)	anal.
20	Me, cyclohexyl	22	C,H,N	61	MeO, Me, Me	1,400	C,H,N
46	*t*-butyl	13	C,H,N	62	cyclohexyl	>400	C,H,N
58	methyl	>7,000	C,H,N	63	Me, tetrahydropyranyl	280	C,H,N
59	*iso*-propyl	330	C,H,N	64	Me, Me, phenyl	760	C,H,N
60	Me, Me, Me	12	C,H,N				

Scheme 2[a]

[a] Reagents: (a) CNCH$_2$CO$_2$H, *n*-BuLi, THF, CH$_2$Cl$_2$, −70 °C and then 25 °C. (b) Phenylhydrazine, toluene, reflux. (c) THF, 25 °C. (d) LDA, THF, MeI, −78 °C. (e) NaH, CH$_3$CN, THF, 75 °C.

target compound **47** was obtained from the sodium cyanoborohydride-mediated reductive hydrazination of cyclohexanone with hydrazine.[47]

Compound **46** was used as a frame of reference for probing the SAR at the 5-position of pyrazole by replacing the *t*-butyl moiety (Table 2). This effort required the construction of a diverse set of oxopentanenitrile subunits. Scheme 2 outlines two general procedures to prepare oxopentanenitrile derivatives. Briefly, the addition of the dianion of cyanoacetic acid[48] to acid chlorides (e.g., **17**) or the anion of acetonitrile[49] to esters (e.g., **22**) supplied the β-keto nitrile components. Following the chemistry described in Scheme 1, pyrazole formation and urea couplings were completed for target **20** as well as the other compounds in Table 2.

To evaluate the role of the urea linkage to the binding of p38, the synthesis of several urea analogues was undertaken. The biological role of each of the urea N−H groups in **16** was examined by replacement with CH$_2$ (**25** and **31**) and *N*-methyl (**34** and **37**). Amides **25** and **31** were prepared as shown in Scheme 3. EDC-mediated condensation of aminopyrazole **15** and 4-chlorophenyl-acetic acid (**24**) furnished amide **25**. Amide **31**, however, required the construction of pyrazole acetic acid **30**. Thus, pyrazolidinone **26** was converted to its O-triflate derivative **27**, which underwent Stille cross coupling with tributyl(vinyl)tin to give vinyl pyrazole **28**. Regioselective hydroboration of **28** produced alcohol **29**, which was converted to the desired carboxylic acid **30** with Jones reagent. Amide bond formation between **30** and 4-chloroaniline with DCC furnished **31**. The syntheses
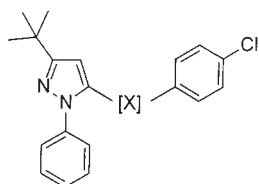
Scheme 3[a]
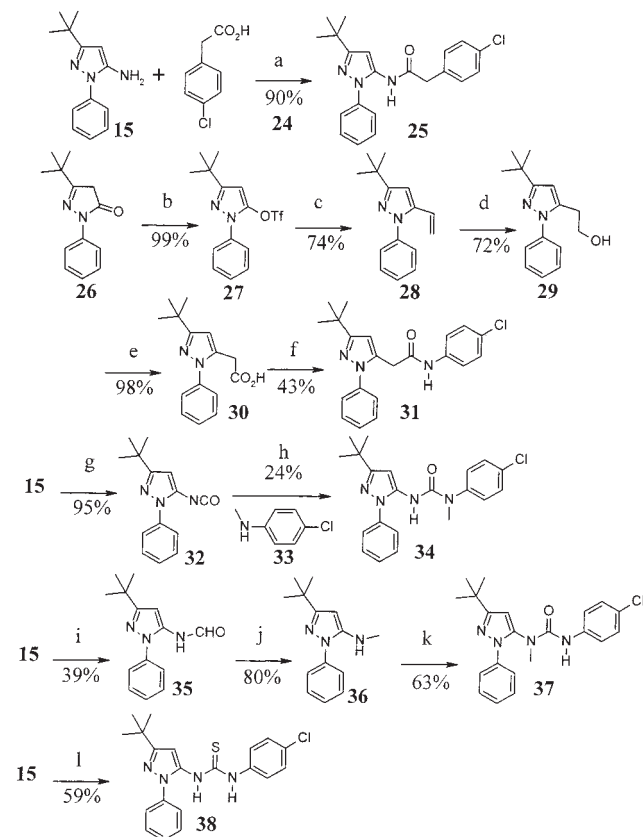
[a] Reagents: (a) EDC, CH$_2$Cl$_2$. (b) Tf$_2$O, DTBMP, CH$_2$Cl$_2$, −78 to 0 °C. (c) Tributyl(vinyl)tin, Pd[P(Ph)$_3$]$_4$, LiCl, dioxane, 100 °C. (d) (i) 9-BBN, THF, reflux. (ii) NaOH, H$_2$O$_2$. (e) Jones reagent. (f) 4-Chloroaniline, DCC, DMAP, CH$_2$Cl$_2$. (g) COCl$_2$, CH$_2$Cl$_2$, aqueous NaHCO$_3$. (h) CH$_2$Cl$_2$, 25 °C. (i) HCO$_2$H, reflux. (j) BH$_3$-DMS, THF, 25 °C. (k) 4-Chlorophenyl isocyanate, CH$_2$Cl$_2$, 25 °C. (l) 4-Chlorophenyl isothiocyanate, CH$_2$Cl$_2$, 25 °C.

produced pyrazole isocyanate **32**, which was coupled with *N*-methyl-4-chloraniline (**33**) to provide *N*-methyl urea **34**. Alternatively, aminopyrazole **15** was heated with formic acid to produce *N*-formyl aminopyrazole **35**, which upon reduction with borane[51] yielded *N*-methyl-aminopyrazole **36**. Treatment of **36** with 4-chlorophenyl isocyanate produced *N*-methyl urea analogue **37**. Thiourea **38** served as a basis to understand the part that the O-atom plays in p38 binding, and its preparation was accomplished by treatment of aminopyrazole **15** with 4-chlorophenyl isothiocyanate.

The compounds designed to explore the region of the urea phenyl of **46** are summarized in Table 4. They were conveniently obtained by the treatment of pyrazole isocyanate **32** with aniline derivatives or alkylamines. For example, as shown in Scheme 4, exposure of isocyanate **32** to 2-aminoindan (**39**) furnished urea **40**. Other target ureas were prepared according to Scheme 1 wherein amine **15** was coupled to aryl isocyanates.
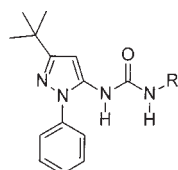
To access target compounds with groups attached to the 4-position of the urea naphthalene, the route shown in Scheme 5 was utilized. Alkylation of *N*-Boc naphthol **41**, prepared from 4-amino-1-naphthol with 4-(2-chloroethyl)morpholine, gave ether **42**. Removal of the Boc protecting group (**43**) and urea formation, as

Table 3. Urea Modifications

compound	[X]	K_d (nM)	anal.
16	NHC(O)NH	8	C,H,N
25	NHC(O)CH$_2$	>900	C,H,N
31	CH$_2$C(O)NH	1,500	C,H,N
34	NHC(O)NCH$_3$	7,500	C,H,N
37	NCH$_3$C(O)NH	>1,000	C,H,N
38	NHC(S)NH	530	C,H,N

Table 4. Modification of Urea-Phenyl Ring

compound	R	K_d (nM)	Inhibition of TNF-α in THP-1 cells EC$_{50}$ (nM)	anal.
46	phenyl	13	730	C,H,N
65	H	>7,000	nd	C,H,N
66	cyclohexyl	130	3,300	C,H,N
67	2-pyridinyl	400	nd[b]	C,H,N
68	3-pyridinyl	420	nd	C,H,N
69	4-pyridinyl	1,200	nd	C,H,N
70	3-NH$_2$-phenyl	100	1,000	C,H,N
71	4-NH$_2$-phenyl	318	nd	C,H,N
72	2,3-dimethylphenyl	3	410	C,H,N
73	CH$_2$-phenyl	47	1,200	C,H,N
74	CH$_2$CH$_2$-phenyl	260	11,000	C,H,N
75	1-naphthyl	5	250	C,H,N
76	2-naphthyl	a	700	C,H,N
40		14	770	C,H,N
77		3	330	C,H,N

a. Compound's fluorescence prevents accurate measurement of K_d.
b. Not determined

Results and Discussion

We recently reported the crystal structure of recombinant human p38 MAP kinase in complex with compound **14** at 2.5 Å resolution (Figure 1).[45] Interestingly, the crystal structure reveals that this compound utilizes binding interactions on the kinase that are spatially distinct from the adenosine 5′-triphosphate (ATP) pocket. There is no structural overlap between the atoms of compound **14** and the ATP (Figure 2). Similarly, there is only limited spatial overlap between **14** and an iodo analogue of SB203580 (**1a**)[52] and this occurs in a lipophilic pocket commonly referred to in the kinase field

Scheme 4[a]
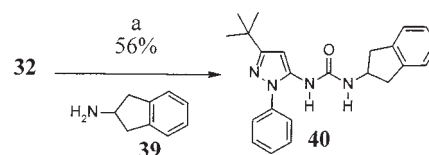
[a] Reagents: (a) CH$_2$Cl$_2$, 25 °C.

Gly170 (DFG) of the kinase is required for the observed binding mode of the diaryl urea inhibitor (Figure 2). In all of the currently known protein Ser/Thr kinase structures, the residues assume a conformation such that the Phe side chain is buried in a hydrophobic pocket in the groove between the two lobes of the kinase (DFG-in conformation). In the structure of the complex with compound **14**, however, the Phe side chain has moved by about 10 Å to a new position (DFG-out conformation). In this position, one face of the Phe side chain and the urea phenyl ring are involved in hydrophobic interactions whereas the other face is exposed to solvent. This movement of the Phe side chain reveals a large hydrophobic domain in the kinase, and the *tert*-butyl group of **14** inserts deep into this pocket (Figure 2). Neither nitrogen atom on the pyrazole ring participates in specific hydrogen-bonding interactions with the kinase. As shown in Figure 3, the urea of **14** establishes a bidentate hydrogen bond with the conserved side chain of Glu71.

Most protein kinase inhibitors use the ATP binding pocket and inhibit the kinase by directly competing with the binding of ATP. In contrast, compound **14** does not compete directly with ATP binding, as it has no structural overlap with the ATP molecule (Figure 2). However, our structure shows that the DFG-out conformation impedes ATP binding, as the side chain of the Phe residue would be sterically incompatible with the phosphate groups of ATP (Figure 2). This is supported by our observation that compound **14** interferes with the inactivation of p38 MAP kinase activity by the fluorescent ATP analogue 5′-*p*-fluorosulfonyl benzoyl adenosine (data not shown). Therefore, the diaryl urea compounds inhibit p38 MAP kinase by stabilizing a conformation of the kinase that is incompatible with ATP binding.

The data in Tables 1 and 2 highlight the binding roles of the groups appended to the pyrazole nucleus of **14**—methyl at N-2 and *tert*-butyl at C-5. Fortuitously, our first modification, replacement of the methyl of **14** with a phenyl group (**16**), improved binding potency 40-fold (Table 1) as measured in a fluorescent binding assay. The crystal structure of **16** and the recombinant human p38 complex (Figure 4) help rationalize this result. The phenyl ring at N-2 of the pyrazole participates in lipophilic interactions with the alkyl portion of the side chain of the Glu71 residue. In addition, the phenyl ring may serve as a water shield for the hydrogen bond network of the urea and the Glu71 carboxylate. The presence of the phenyl ring causes this Glu residue to adopt a side chain conformation that results in a monodentate hydrogen-bonding interaction with the urea moiety of the inhibitor. This alignment of Glu71 is in contrast to the bidentate interactions in the complex with **14** (Figure 3).

Scheme 5[a]
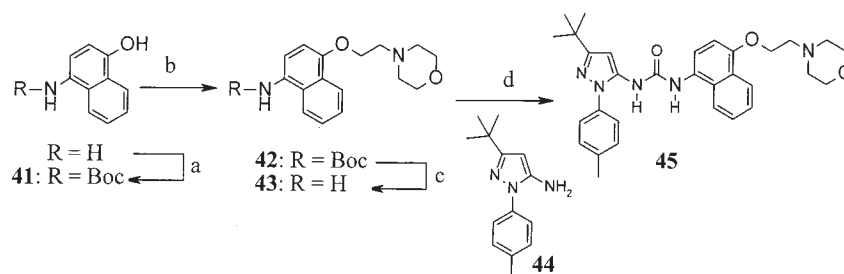
[a] Reagents: (a) Di-*tert*-butyl dicarbonate, THF, 25 °C. (b) 4-(2-Chloroethyl)morpholine, K_2CO_3, acetonitrile, heat. (c) HCl, dioxane. (d) Compound **44**, phosgene, THF.
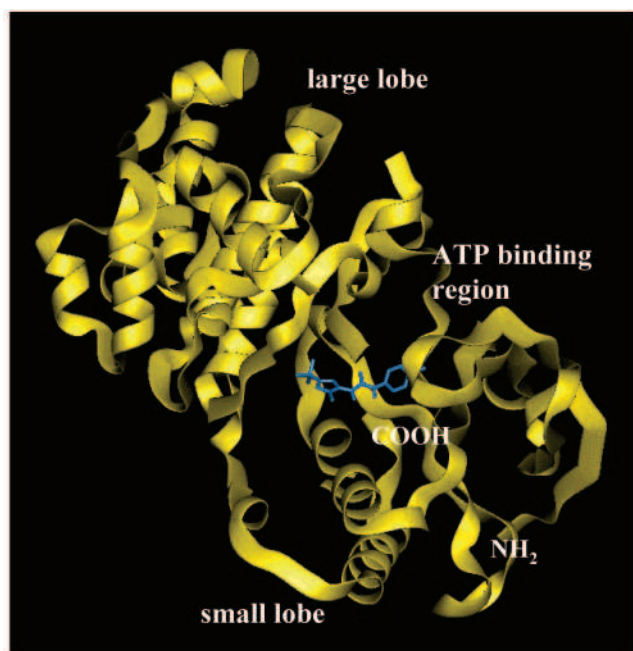

Figure 1. Crystal structure of human p38 MAP kinase and **14** at 2.5 Å resolution.

Figure 2. Overlap of **14** (blue) and ATP (red). The urea hydrogen atoms are shown for clarity. Phe169 is shown in red when occupying the DFG-in conformation (ATP bound) and in blue in the DFG-out conformation when **14** is bound to p38.

pyrazole and confirmed our hypothesis regarding binding interactions at this domain. The diminished potency of saturated derivative **47** highlighted the necessity for an aromatic ring to achieve optimal hydrophobic interactions (Table 1). Addition of methyl groups to the 3- and 4-position of the phenyl ring of **46** provided modest improvements in binding (**49**−**51**). However, 2-methyl derivative **48** displayed a substantial loss of binding affinity possibly due to an increase in the torsional angle favored between the phenyl and the pyrazole rings beyond the observed angle of 54° for **16** (Figure 4). This position tolerates bulkier groups as judged by the binding potency of 2-naphthyl analogue **52**. In addition, heteroatoms (**53**−**57**) can be accommodated at this site. The close proximity of the 3- and 4-positions of the phenyl ring of **46** to solvent may explain these results.

In Figure 4, the *tert*-butyl group at C-5 of pyrazole **16** is embedded deep into a hydrophobic pocket formed by the reorganization of Phe169 in the DFG-out conformation. In an effort to understand the binding role of the *tert*-butyl moiety in this class of compounds, we investigated the size and electronic requirements of this group. As can be seen in Table 2, removal of one methyl
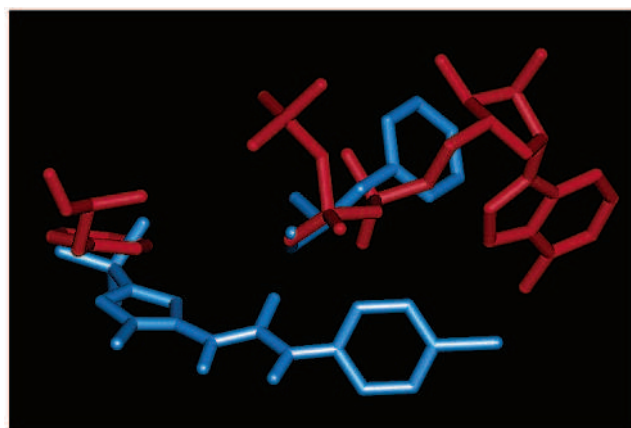
compound (**58**). This lipophilic binding pocket tolerated bulkier *tert*-alkyl groups such as dimethylethyl (**60**) and methylcyclohexyl (**20**). However, the 50-fold loss of binding observed with dimethylbenzyl analogue **64** may indicate a size limitation for this domain. A comparison of cyclohexyl derivatives **62** and **20** further exemplifies the strong preference for a tertiary group. The relatively poor activity of compounds **61** and **63** as compared to **60** and **20** suggest that lipophilic substitution at C-5 of the pyrazole is favored. Taken together, these results are rationalizable based on the crystal structure of **16** and p38 (Figure 4) that indicate a lipophilic group at C-5 of the pyrazole has important hydrophobic binding interactions with the protein in the DFG-out conformation. The *tert*-butyl group was incorporated into all subsequent target molecules since it offered the best balance of potency and physicochemical properties.

The X-ray crystallographic structure of **16** with p38 reveals a hydrogen bond network consisting of a urea hydrogen and the carboxylate oxygen of Glu71 and also the urea oxygen and N−H of Asp168. The data in Table 3 highlight the significance of these interactions on binding affinity. Replacement of either N−H in the urea with a methylene group (compounds **25** and **31**) or introduction of *N*-methyl (**34** and **37**) results in significant loss of activity. Likewise, the thiourea analogue **38** shows a 60-fold decrease in binding potency to p38 as compared to **16**. These findings underscore the crucial contribution that the urea makes to binding with p38 through extensive hydrogen bonding and, also likely,

Explore Litigation Insights

DOCKET ALARM

Docket Alarm provides insights to develop a more informed litigation strategy and the peace of mind of knowing you're on top of things.

Real-Time Litigation Alerts

Keep your litigation team up-to-date with **real-time alerts** and advanced team management tools built for the enterprise, all while greatly reducing PACER spend.

Our comprehensive service means we can handle Federal, State, and Administrative courts across the country.

Advanced Docket Research

With over 230 million records, Docket Alarm's cloud-native docket research platform finds what other services can't. Coverage includes Federal, State, plus PTAB, TTAB, ITC and NLRB decisions, all in one place.

Identify arguments that have been successful in the past with full text, pinpoint searching. Link to case law cited within any court document via Fastcase.

Analytics At Your Fingertips

Learn what happened the last time a particular judge, opposing counsel or company faced cases similar to yours.

Advanced out-of-the-box PTAB and TTAB analytics are always at your fingertips.

API

Docket Alarm offers a powerful API (application programming interface) to developers that want to integrate case filings into their apps.

LAW FIRMS

Build custom dashboards for your attorneys and clients with live data direct from the court.

Automate many repetitive legal tasks like conflict checks, document management, and marketing.

FINANCIAL INSTITUTIONS

Litigation and bankruptcy checks for companies and debtors.

E-DISCOVERY AND LEGAL VENDORS

Sync your system to PACER to automate legal marketing.

fastcase®
Smarter legal research.